J Fluoresc (2006) 16:411–421
DOI 10.1007/s10895-006-0090-z

ORIGINAL PAPER

Nanocrystalline RE_2O_3:Tm^{3+} (RE: Gd^{3+}, Y^{3+}) Blue Phosphors Synthesized via the Combustion Method

Janaína Gomes · Ana Maria Pires · Osvaldo Antonio Serra

Received: 1 November 2005 / Accepted: 27 February 2006 / Published online: 12 May 2006

Abstract This work reports on the preparation of a luminescent blue-emitting rare earth (RE) Tm-doped oxide phosphor. Nanocrystalline RE_2O_3:Tm^{3+} particles were prepared via the combustion method using citric acid, glycine, or urea as fuels. Samples were doped with different percentages of the activator Tm^{3+}. The post-annealing treatment was performed in air for all the samples, at temperatures ranging from 800 to 1100°C, for 4 h. The samples were characterized by X-ray diffraction (XRD), photoluminescence spectroscopy (PL) and scanning electron and transmission microscopies (SEM and TEM) in order to determine the best synthetic procedure. The post-annealed powders showed blue emission with maximum at 452 nm characteristics for Tm^{3+} transition $^1D_2 \rightarrow {}^3H_4$ (under UV excitation at 360 nm). Samples, presented a tri-dimensional porous structure (50–200 nm) formed of spheroid particles with a diameter between 20 and 60 nm. The best luminescent material was obtained when urea was used to prepare nanoparticles of Gd_2O_3 doped with 0.5% Tm^{3+}, and 1100°C was used as the post-annealing temperature.

Keywords Blue phosphor · Yttrium · Thulium · Gadolinium · Combustion method

Introduction

Nanosized particles have been intensively studied in recent years because their properties significantly differ from those of the corresponding bulk compounds. Most of the research efforts have been devoted to optical properties induced by quantum confinement, and it is expected that nanoparticles can act as potential luminescent materials for both fundamental research and applications [1]. Rare earth ions are good activators for luminescent materials, so oxide phosphors have recently gained much attention since they can be applied in plasma panel screens (PDP) and field emission (FED) displays, as well as in white color light-emitting diodes. In fact, the chemical stability of oxide phosphors is higher than that of sulfide phosphors [2]. However, Tm^{3+}-activated phosphors in the powder form are not yet in practical use in any emissive displays and must be investigated more thoroughly. There is a significant research interest in the development of Y_2O_3:Eu^{3+} phosphor for FED applications because of its simple host structure and efficient luminescence. The advantages of thinner phosphor screens are their improved conduction, light transmission and 3D resolution, reduced saturation effects, better thermal stability, reduced outgassing, better adhesion to solid surfaces, and good heat resistance [3]. So this work reports on the preparation of a highly luminescent blue-emitting Tm^{3+}-doped oxide. In this context, we have investigated Tm^{3+}-activated RE_2O_3 (RE: Gd^{3+}, Y^{3+}) as a potential blue emitting phosphor for FED applications.

Experimental

Nanosized RE_2O_3 consisting of $Gd(NO_3)_3$ (Strem Chemicals) or $Y(NO_3)_3$,[1] both doped with 0.25, 0.50, and 1.00 mol% of $Tm(NO_3)_3$[1], were prepared using a combustion synthesis [4] procedure. Rare earth nitrates [5, 6] and

J. Gomes · A. M. Pires · O. A. Serra
Laboratório de Terras Raras, Departamento de Química, Faculdade de Filosofia Ciências e Letras de Ribeirão Preto, Universidade de São Paulo, Brasil

J. Gomes (✉)
Av Bandeirantes, 3900 Ribeirão Preto, SP, 14040-901, Brazil
e-mail: jangomes@usp.br

[1] Y_2O_3 99.99% and Tm_2O_3 99.99% was kindly provided by Dr. Jun Lin, Changchun, China.

citric acid were mixed together in a porcelain crucible, in the desired ratio, to form the precursor solution. Excess water was evaporated, condensing the precursor solution while heating. As the ignition occurred, the reaction went on vigorously for a few seconds. A fluffy product was obtained after the combustion reaction. Glycine and urea were also used as fuels for comparison. Post-annealing was performed for all the samples prepared as above, in a muffle furnace for 4 h, in the temperature range 800–1100°C which favours the RE_2O_3 crystalline phase formation [7].

The crystalline structures of the phosphors were investigated by X-ray diffraction (XRD) in a SIEMENS D5000 diffractometer, K_α Cu radiation, $\lambda = 1.5418$ Å, equipped with a graphite monochromator. The photoluminescence (PL) properties at room temperature were evaluated using a spectrofluorometer FLUOROLOG3 ISA/Jobin-Yvon, 450 W ozone free Xenon lamp, equipped with a Hamamatsu R928P photomultiplier. Kinetic measurements were performed by using the same spectrofluorometer equipped with a Xenon pulsed lamp and a phosphorimeter 1934 D. Scanning electron microscopy (SEM) was performed in a Zeiss D5M960 microscope, in order to characterize particle morphology. In this case, samples were first dispersed in acetone and dropped over a metallic holder, which was coated with a gold film, in a deposition controlled by a Sputter Coater Baltec SCD 050. Transmission electron microscopy, TEM was also performed for two chosen samples in order to achieve higher magnification by using a Philips CM200 transmission microscope, equipped with a Digital Spectrometer – Prism PGT – Princeton Gamma Tech; the image aquisition was performed by using two Soft Imaging System Cameras (KeenView model, 1.5 Mpixels; Morada model, 11 Mpixels). The selected-area electron-diffraction (SAED) pattern of the individual nanoparticles was obtained during TEM measurements in order to evaluate their crystalline nature. In the case of TEM measurements, powder sample was suspended in ethanol absolute and supported in a copper grid.

Results and discussion

Photoluminescence spectroscopy (PL)

The typical photoluminescence emission spectra under a 360 nm excitation of RE_2O_3:Tm^{3+} (RE: Gd^{3+}, Y^{3+}) samples prepared from different fuels, with varying activator concentration (0.25–1 mol% of Tm^{3+}) at different post-annealing temperatures (800–1100°C) are shown in Figs. 1, 2, 4, 5 and 7. The doping concentration range of Tm^{3+} was chosen based in previously reported Tm^{3+} activated phosphor's preparation [8], whereas it was observed a Tm^{3+} self quenching at doping concentrations higher than 1%.

For all prepared phosphors, independently of the host lattice, the emission observed in the 445–470 nm blue range is ascribed to $^1D_2 \rightarrow {}^3H_4$ Tm^{3+} transition [9]. The number of peaks viewed for this transition ($^1D_2 \rightarrow {}^3H_4$) varies as a function of the employed fuel. These photoluminescence results were used to evaluate the optimium activator concentration and the best annealing temperature based on the comparison of the qualitative emission intensity.

Therefore, the relative emission intensities estimated from Gd_2O_3 doped phosphors emission spectra, Fig. 1, were compared to find out the optimum Tm^{3+} concentration. Considering each doping ion concentration for each employed fuel, the relative emission intensity was used to point out the higher intensity luminescence among the samples prepared under different post-annealing temperatures. These results were summarized in Table 1.

The analysis of gadollinium doped samples emission spectra, Figs. 1 and 2, reveals at least five well-defined peaks, with maxima at 447, 453, 457, 459, and 463 nm. Samples prepared with glycine show a different profile when compared to the other ones, but the number of defined peaks remains the same. By using the values summarized in Table 1, it is possible to observe a significant difference in the emission intensity, which in general increases with increasing activator concentration, considering the best post-annealing temperature in each case. However, the emission intensity of the sample using urea does not increase with increasing activator concentration. After 0.50 mol% of Tm^{3+}, there is a concentration quenching, which could be related to the doping ion distribution in this powder that is influenced by the final structure achieved by using such fuel. This aspect will be better discussed latter.

Finally, for a systematic study, the most intense emission curves were plotted together in Fig. 2, in order to determine which arrangement of fuel and activator concentration yielded the most intense phosphor. As can be noted, the phosphor with 0.50 mol% of Tm^{3+} prepared from urea with post-annealing of 1100°C presents higher intensity than those prepared from the other fuels.

Excitation spectra were also performed for all the samples ($\lambda_{emission} = 453$ nm), and the same broad band assigned to $^3H_6 \rightarrow {}^1D_2$ transition with maximum at 363 nm is observed. A representative spectrum is shown in Fig. 3.

The same procedure adopted for the Gd_2O_3:Tm^{3+} samples were taken to find out the optimum Tm^{3+} concentration for all the Y_2O_3:Tm^{3+} samples, Figs. 4–7.

In Table 1, it is also included data evaluated from the emission spectra obtained for each concentration doping ion and post-annealing treatment used in Y_2O_3 samples. As observed in the case of gadolinium phosphors, the spectra display the same five peaks with maxima at 447, 453, 457, 459, and 463 nm. The emission intensity increases with increasing activator concentration, except for samples using citric

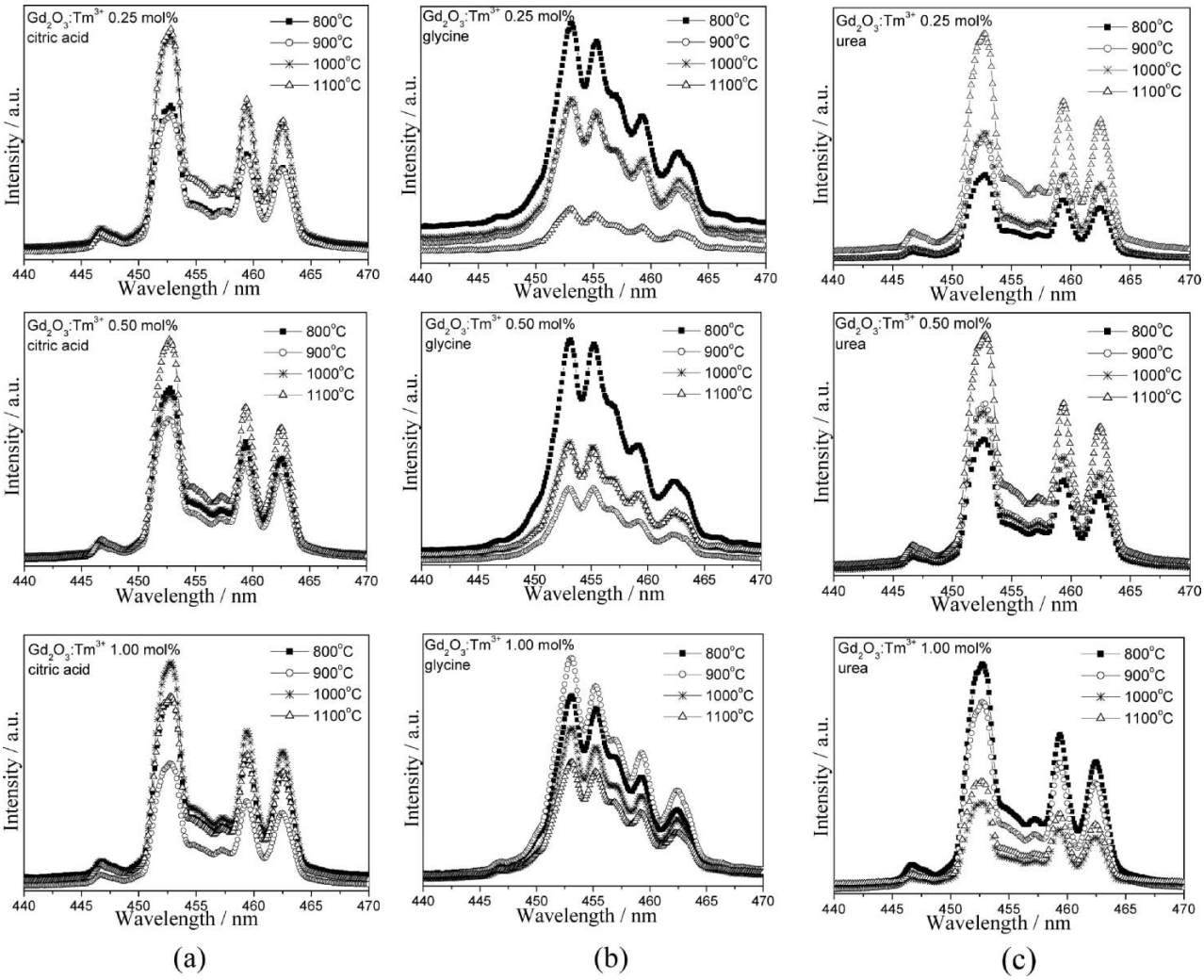

Fig. 1 Emission spectra at room temperature ($\lambda_{ex} = 360$ nm) of Gd_2O_3:Tm^{3+} prepared from the combustion precusor method by using (**a**) citric acid, (**b**) glycine, or (**c**) urea as fuel, post-annealing temperature 800–1100°C, for 4 h

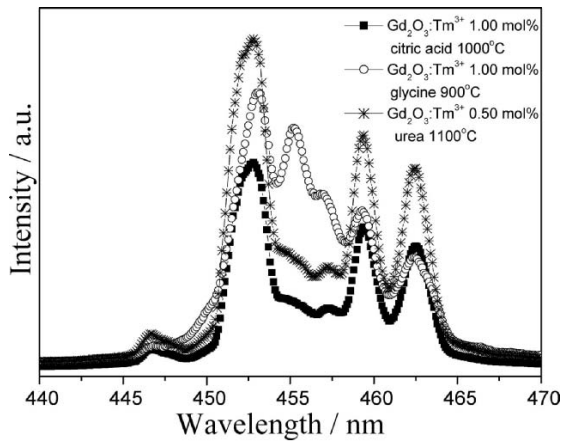

Fig. 2 Emission spectra at room temperature ($\lambda_{ex} = 360$ nm) of Gd_2O_3:Tm^{3+} prepared by the precusor combustion method using citric acid, glycine, or urea as fuels, at different post-annealing temperatures and different concentrations of doping ion

acid, which after 0.50 mol% of Tm^{3+}, presents concentration quenching. Once again, for a systematic study, the curves that presented the most intense emissions were plotted together, Fig. 5, to determine which fuel and which activator concentration yielded the most intense yttrium phosphor. As can be noted, phosphor with 1.00 mol% Tm^{3+} from urea prepared with post-annealing of 800°C presents higher intensity than those obtained from other fuels.

Excitation spectra were also performed for all yttrium samples and the same broad band with maximum at ~ 363 nm was observed; a representative spectrum is shown in Fig. 6.

When the emission intensity of both most intense Tm-doped host lattices is compared, Fig. 7, it is possible to observe that the sample containing gadolinium exhibits the most intense emission. Therefore, concearning these study of emission intensity properties, the best conditions to prepared

Table 1 Relative emission intensity evaluated from emission spectra under 360 nm excitation (Figs. 1–7) used to estimate the higher intensity luminescence among the RE_2O_3:Tm^{3+} samples for each fuel

Fuel	Tm^{3+} (mol%)	Gd_2O_3 samples		Y_2O_3 samples	
		T (°C)	Emission intensity[a]	T (°C)	Emission intensity[a]
Citric acid	1.00	1000	115585	1100	35811
	0.50	1100	105583	900	52023
	0.25	1000	74150	1000	22885
Glycine	1.00	900	154305	900	65575
	0.50	800	105727	900	52878
	0.25	800	73989	800	24826
Urea	1.00	800	141735	**800**	**104922**
	0.50	**1100**	**182884**	800	62859
	0.25	1100	129543	900	50590

[a] $\lambda = 452$ nm (cps).

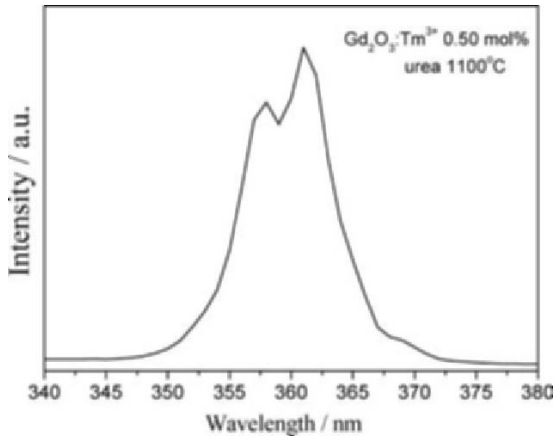

Fig. 3 Excitation spectra at room temperature ($\lambda_{em} = 453$ nm) of Gd_2O_3:Tm^{3+} 0.50 mol% prepared by the precusor combustion method using urea as fuel at a post-annealing temperature of 1100°C for 4 h

a blue phosphor from combustion method are: Tm^{3+} doping ion concentration of 0.50 mol%, post-annealing treatment at 1100°C for 4 hr, urea as fuel, and gadolinium as host cation.

It is well known that the chemical stability of oxide phosphors is higher than that of sulfide ones applied in image displays [2]. Therefore, the blue emitting degradation of the phosphors reported in this work is minimal, since displays run at higher temperatures than room temperature. For display operations the decay time is another important factor that should not exceed 10% original light output [10]. Consequently, kinectics measurements were performed, and it is observed that the lifetime decay related to 452 nm emission is 34 μs for Tm-doped gadolinium samples and 35 μs for yttrium ones. The time of emission persistence after the interruption of excitation source does not exceed 100 μs in all cases.

Quantum yield measurements [11] were obtained for the two most intense RE_2O_3:Tm^{3+} prepared samples, by comparison with an industrial standard phosphor, i.e., ZnS:Ag (quantum yield $\sim$0.1) [12]. The samples Gd_2O_3:Tm^{3+} (0.5%) and Y_2O_3:Tm^{3+}(1.00%) from urea and post-annealing temperature at 1100 and 800°C, respectively, comparatively to the ZnS:Ag present a quantum yield $\sim$10 times less. Although the quantum yield (0.01) for the prepared samples are lower than standard blue phosphor, factors low persistence and good stability corroborate to phosphor's display aplications.

Table 2 Mean crystallite size obtained from XRD data (Fig. 8) for the gadolinium and yttrium samples prepared using urea as fuel at different post-annealing temperatures and activator concentration

Host	Tm^{3+} (mol%)	Post-annealing temperature (°C)	Mean crystallite size (nm)
Gd_2O_3	0.25	1100	33
	0.50	1100	36
	1.00	800	27
Y_2O_3	0.25	900	21
	0.50	800	20
	1.00	800	19

X-Ray diffraction (XRD)

On the basis of the photoluminescent results discussed before, the most representative RE_2O_3:Tm^{3+} samples were selected to be characterized by XRD. The XRD patterns of the samples prepared from different fuels under the optimized conditions, to yield the most intense luminescence emission spectra, are shown in Fig. 8. It is possible to verify, Fig. 8, the formation of a Gd_2O_3 single-phase for samples containing gadolinium as host.

The crystallite size of all samples characterized by XRD, which diffraction patterns are viewed in Fig. 8, was estimated from the half-width of the detected Gd_2O_3 and Y_2O_3 single-phases reflection peaks by using the Scherrer's equation [14] and are listed in Table 2. The average crystallite size for the Gd_2O_3:Tm^{3+} samples lies between 27 and 36 nm and for the Y_2O_3:Tm^{3+} ones between 19 and 21 nm. In the case of Gd phosphors, the influence of annealing temperature is evident because the sample heated at 800°C shows the lower crystallite mean size. When samples are annealed at 1100°C there is enough energy to favour the crystallite growth. This behavior is not observed for Y analized phosphors, because the choosen samples were post-annealed at lower temperatures, providing similar mean crystallite sizes among themselves.

Chromaticity (CIE)

Basic requirements for display phosphors are stability and emission color purity [15] according to the standard set by

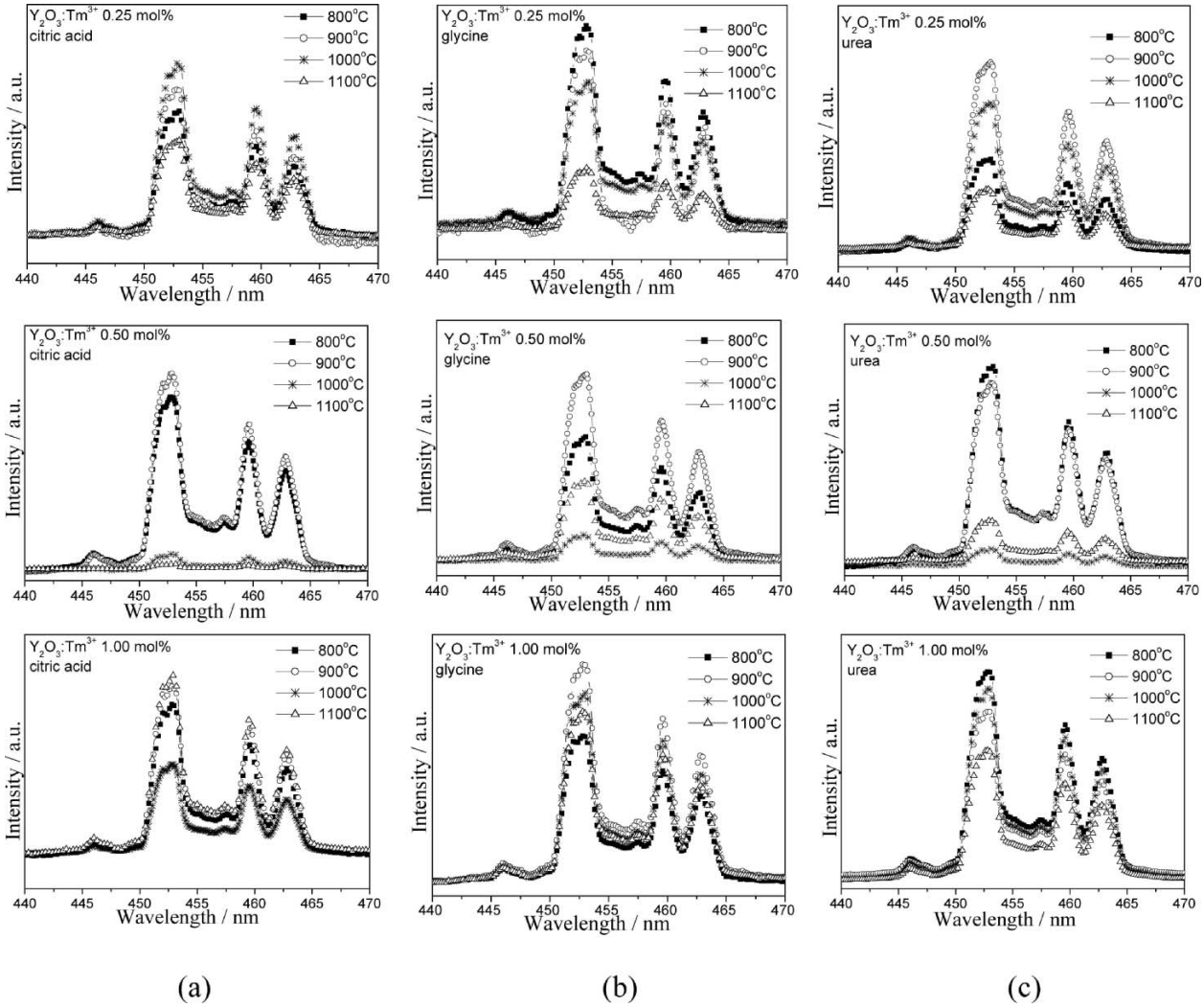

Fig. 4 Emission spectra at room temperature ($\lambda_{ex} = 360$ nm) of Y_2O_3:Tm^{3+} prepared by the precusor combustion method using (**a**) citric acid, (**b**) glycine, or (**c**) urea as fuel, post-annealing temperature of 800–1100°C for 4 h

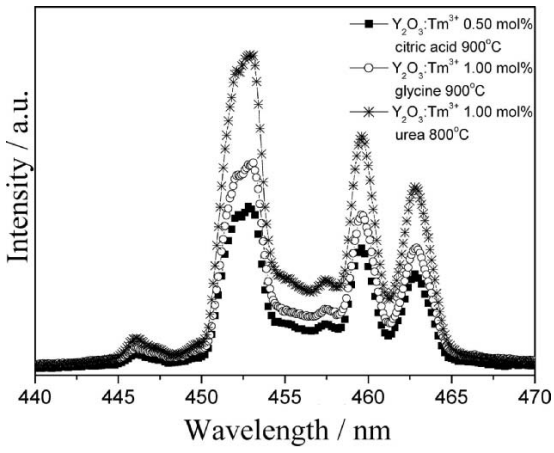

Fig. 5 Emission spectra at room temperature ($\lambda_{ex} = 360$ nm) of Y_2O_3:Tm^{3+} prepared by the precusor combustion method using citric acid, glycine, or urea as fuels, at different post-annealing temperatures and different concentration of doping

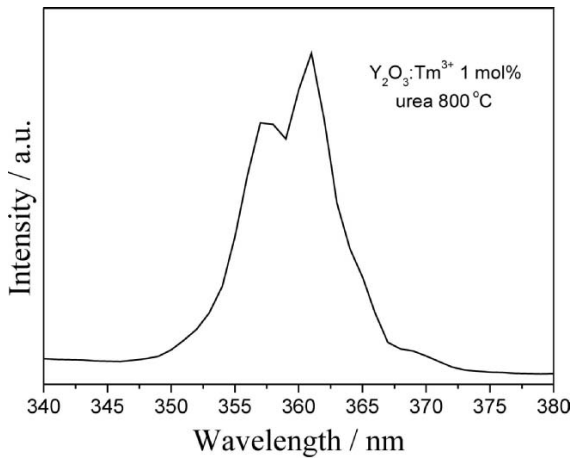

Fig. 6 Excitation spectra at room temperature ($\lambda_{ex} = 453$ nm) of Y_2O_3:Tm^{3+} 1.00 mol% prepared by the precusor combustion method using glycine as fuel at 800°C, post-annealing temperature for 4 h

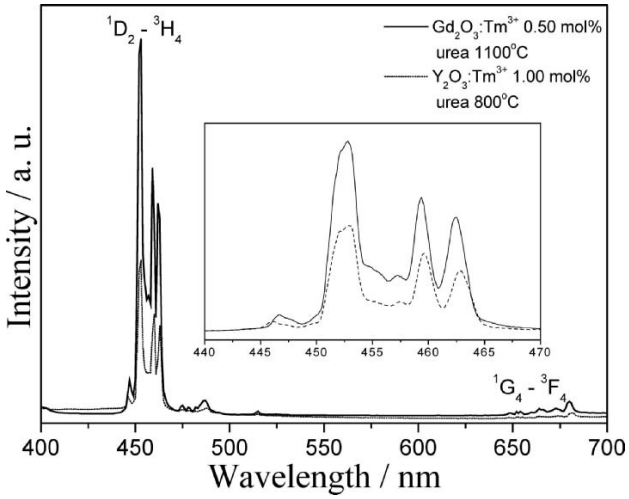

Fig. 7 Emission spectra at room temperature ($\lambda_{ex} = 360$ nm) of Y_2O_3:Tm^{3+} prepared by the precusor combustion method using urea as fuel at different post-annealing temperatures and different concentrations of dopings

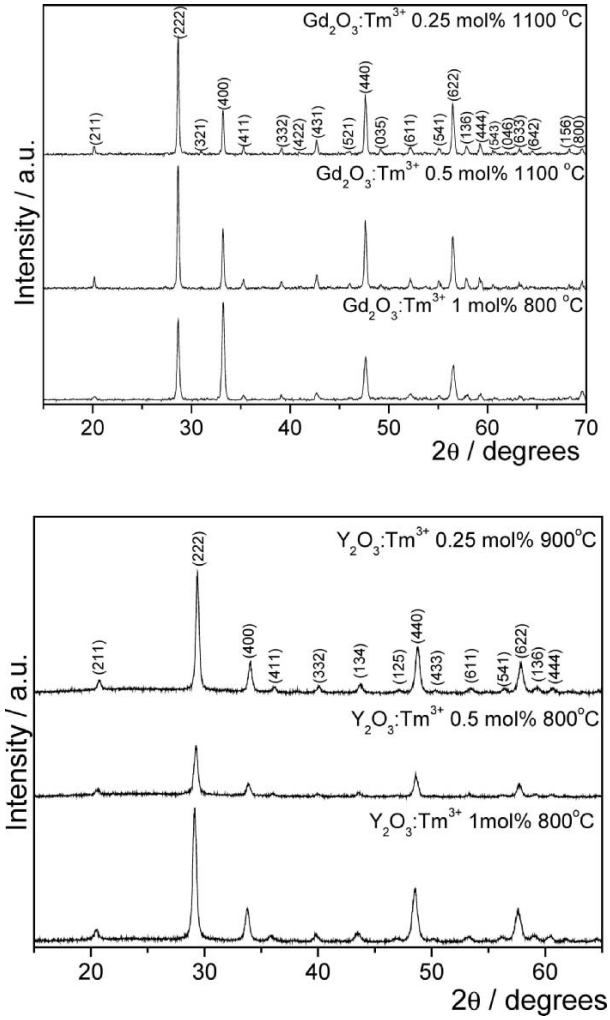

Fig. 8 XRD patterns recorded for Gd_2O_3:Tm^{3+} (PDF n. 76-0155 [12]) and Y_2O_3:Tm^{3+} (PDF n. 86-1326 [13]) samples prepared at different activator concentrations by the precursor combustion method using urea as fuel at different post-annealing treatment

EBU (European Broadcasting Union). Color purity can be visualized in the chromaticity diagram, as blue, red, and green regions, with the emission color coordinates of the luminescent material. Therefore, the chromaticity diagrams as well as the respective chromaticity coordinates were obtained from the luminescence emission spectra of some representative RE_2O_3:Tm^{3+} samples, by using a Spectra Lux Software v.2.0 Beta [16]. In Fig. 9a, the chromaticity diagram of the most intense luminescent emission spectra obtained from the gadolinium samples using different fuels are compared, and the same comparison is displayed for yttrium phosphors in Fig. 9b. For both types of phosphors, analysis of the chromaticity diagram is in agreement with the previously discussed results; i.e., the Gd_2O_3 sample doped with 0.50 mol% Tm^{3+} obtained from urea at 1100°C, and the Y_2O_3 sample doped with 1.00 mol% Tm^{3+} obtained from urea at 1100°C present the most adequate color coordinates, Table 3, according to the EBU standard for a blue display phosphor ($y < 0.072$ and $x > 0.143$).

In Fig. 10, the chromaticity diagram of the most samples intense luminescence emission spectra, obtained from samples using urea as fuel, and containing different host lattices (gadolinium and yttrium) are shown for comparison. Once again the gadolinium sample presents the best color coordinates for a blue display phosphor, confirming that this sample exhibits the best desired optical and structural properties.

Table 3 Chromaticity Coordinates Obtained for the Gadolinium and Yttrium Samples Exhibiting the Most Intense Luminescence for Each Fuel

Host	Fuel	*X*	*Y*	*Z*
Gd_2O_3	Citric acid	0.20	0.08	0.73
	Glycine	0.20	0.08	0.73
	Urea	0.20	0.07	0.73
Y_2O_3	Citric acid	0.22	0.13	0.65
	Glycine	0.22	0.12	0.66
	Urea	0.20	0.14	0.66

Scanning electron microscopy (SEM)

The SEM images viewed in Figs. 11 and 12 of the same samples chosen for characterization by CIE show the general morphological aspect of the powder particles. It is possible to observe that samples obtained by the combustion method, present spheroid particles, with a diameter between 25 and 50 nm, independently of the employed fuel, that form agglomerates in a fractal sponge-like structure, with diameters ranging between 100 and 200 nm. It is important to note that when urea is employed as fuel, the particles seem to be more consolidated than those obtained in the other cases. These

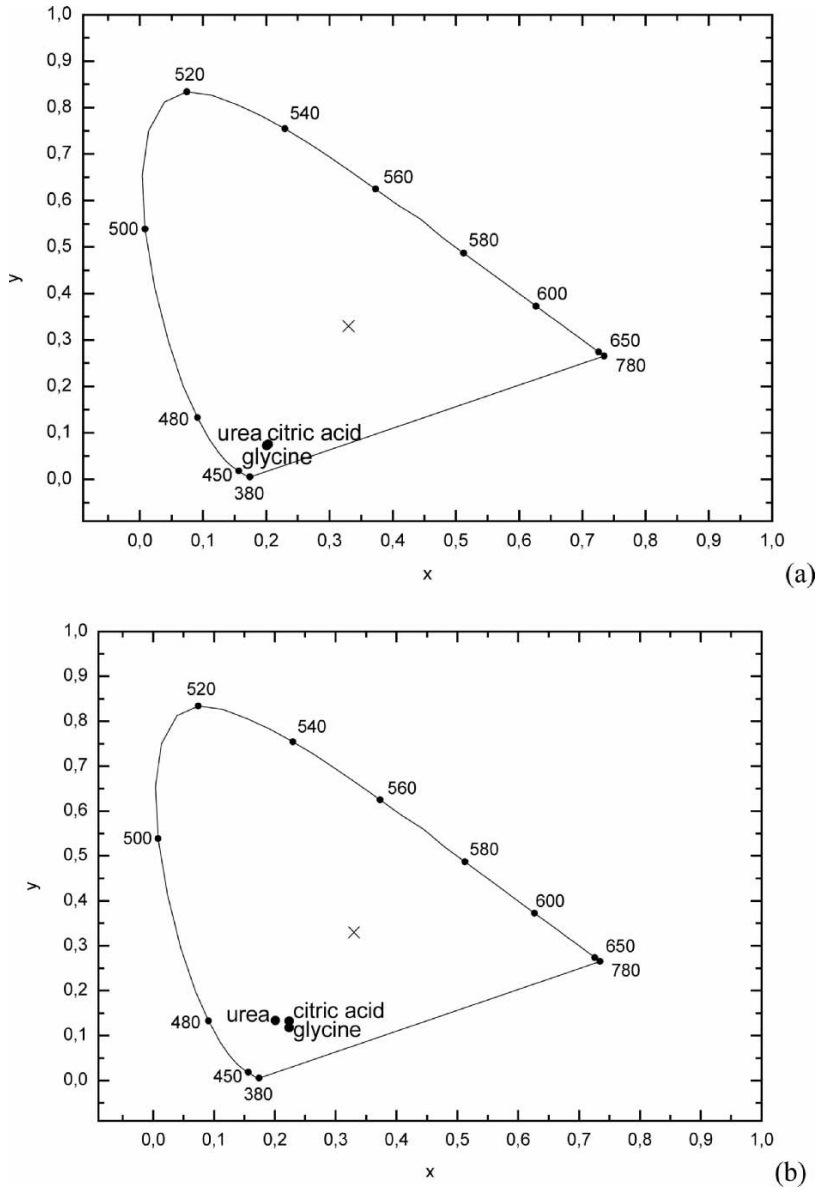

Fig. 9 Chromaticity diagram for the most intense luminescent (**a**) gadolinium and (**b**) yttrium samples obtained for each fuel

results are in agreement with data obtained from XRD (crystallite size between 15 and 40 nm), and confirm that post-annealing at higher temperatures can grow nanoparticles into larger isolated agglomerates. Moreover, the high temperature is also necessary and important to improve luminescent intensity. When nanoparticles or small-sized systems are taken into account, the presence of CO_3^{2-} and OH^- groups with high frequency vibrational modes on the surface of the particles increases as the particle size decreases [17]. The higher frequencies can induce other non-radiative relaxations for Tm^{3+}, leading to PL quenching.

Transmission electron microscopy (TEM)

In order to confirm both XRD and SEM information, TEM images with higher resolution were obtained and are viewed in Fig. 13 for the two most intense samples. First, for both samples, a panoramic image is provided showing that particles are arranged in a sponge-like ordely structure, mainly in the case of Y-sample. Y-sample presents particles with 20 nm diameter size, but for Gd-sample it is very difficult to define particles boundary due to temperature effect, that initiate a sintering process. This fact is in agreement with XRD results discussed before. The porous varies between 50 and 200 nm, and SAED pattern of the individual nanoparticles included in Fig. 13 ensure their crystalline nature. The profile viewed for Y-sample is much richer in details, showing a superposition of regular lattices probably due to an effect of the sponge-like ordely structure. SAED pattern of Gd-sample also displays a regular crystalline profile, but not superposed, because once again the higher post-annealing temperature lead to a more

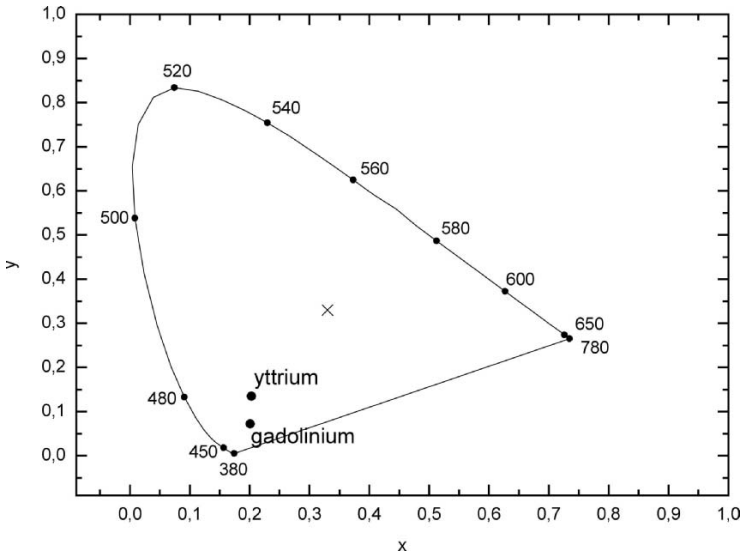

Fig. 10 Chromaticity diagram obtained from samples $RE_2O_3:Tm^{3+}$

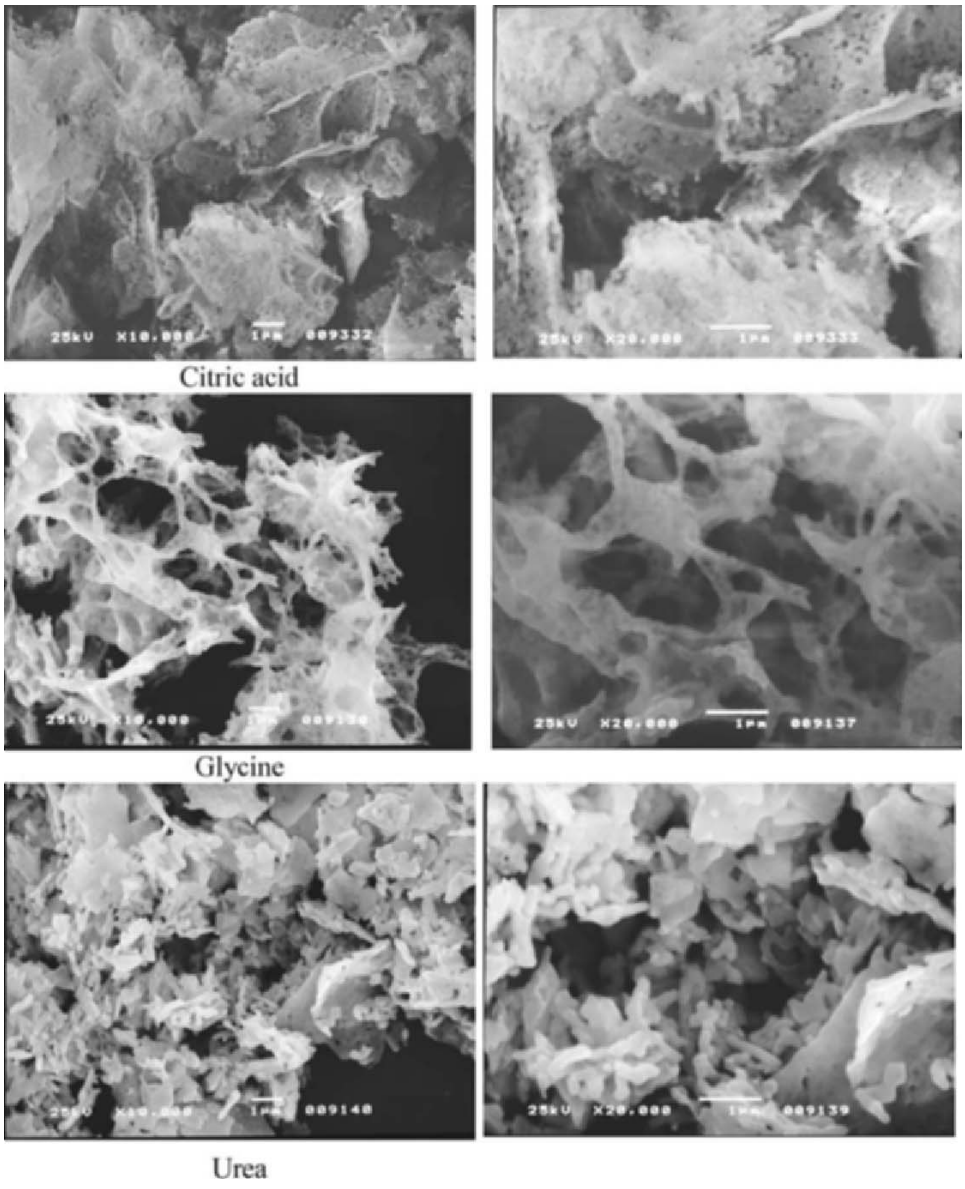

Fig. 11 SEM of $Gd_2O_3:Tm^{3+}$ prepared by the combustion method

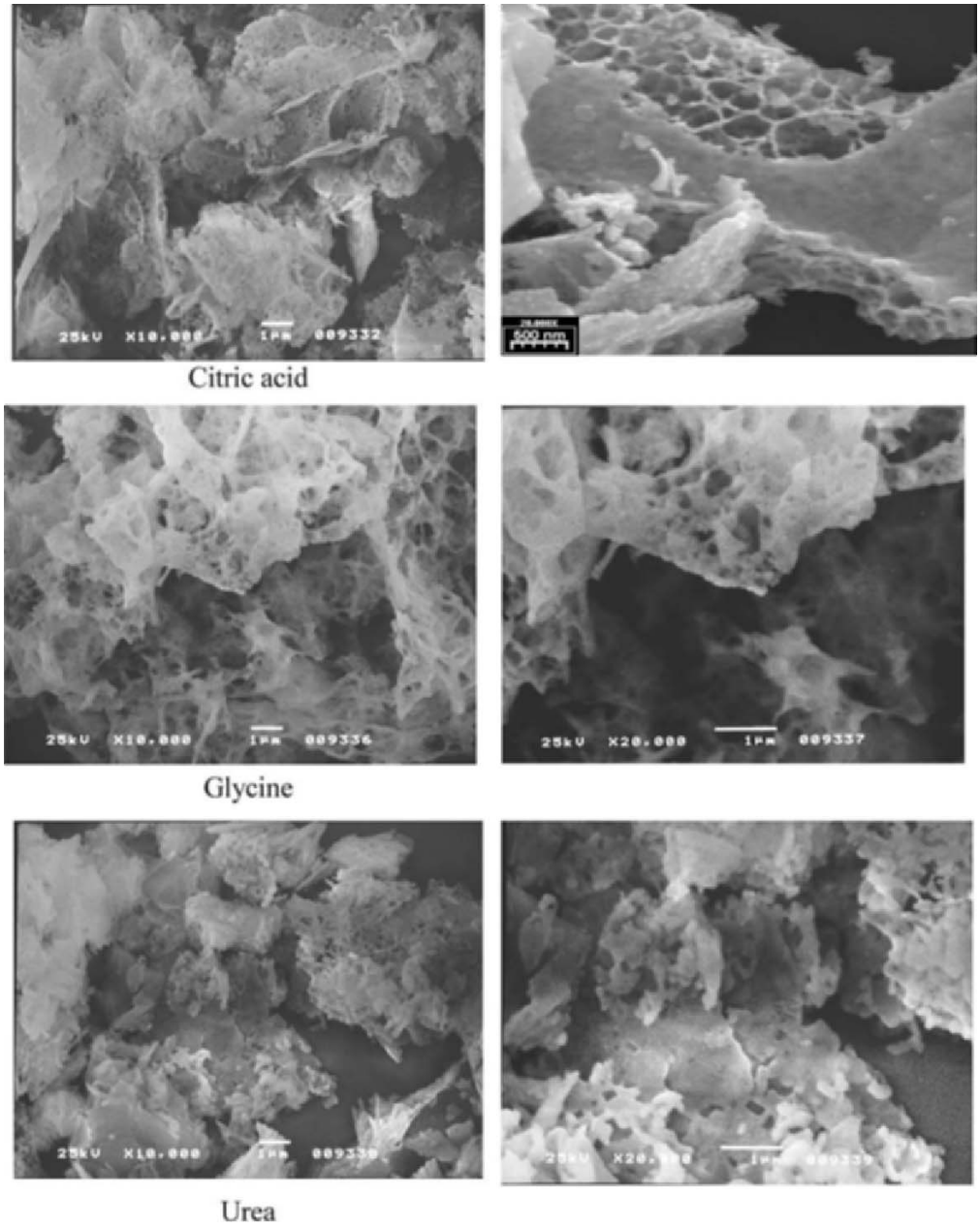

Fig. 12 SEM of Y_2O_3:Tm^{3+} prepared by the combustion method

consolidate nanostructure. These results are in agreement with the others techniques and helped to refine the already obtained results.

Conclusions

In summary, the synthesis of RE_2O_3:Tm^{3+} blue nanophosphors with PL emission was achieved via the combustion method. The diffraction peaks obtained for such phosphors are very well defined. The nanoparticles size is in the range of 20 nm, and they form agglomerates with a diameter ranging from 50 to 200 nm. The photoluminescence properties of both type of phosphors (containing either Gd or Y) exhibit the typical fluorescence of the Tm^{3+} ion, independent of the fuel employed. Our results suggest that among the obtained phosphors, the ones that exhibits higher photoluminescence intensity in the blue region ($\sim$452 nm) upon UV excitation at 360 nm can be prepared with urea as fuel, post-annealing temperature at 1100 and 800°C, 0.50 and 1.00% mol of Tm^{3+}, for Gd and Y host lattices, respectively. Comparing the luminescence intensities of these two samples, Gd_2O_3:Tm^{3+} 0.50 mol% displays the best luminescence. However, Y_2O_3 can still be considered as a feasible matrix because of its higher availability and lower price. The chromaticity coordinates (0.20, 0.07, and

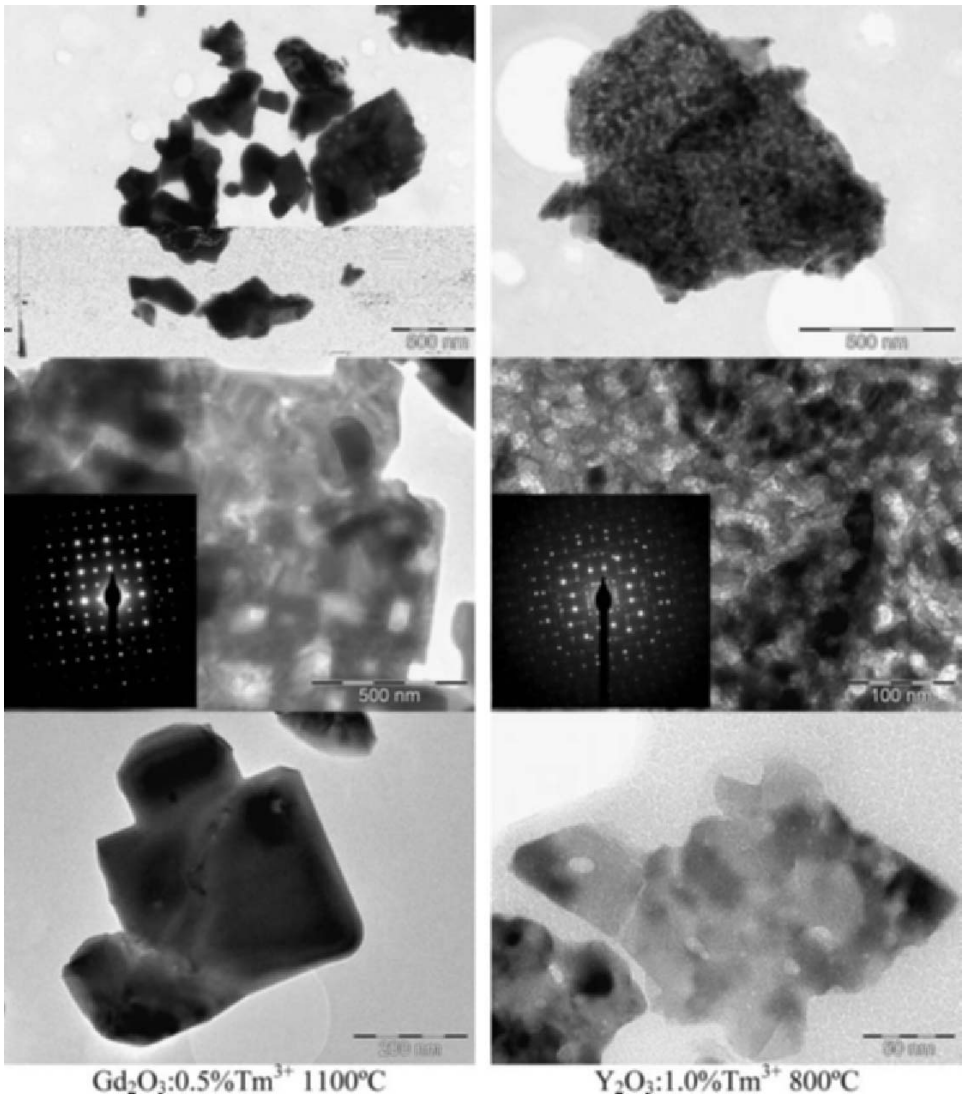

Fig. 13 TEM of RE_2O_3:Tm^{3+} prepared by the combustion method using urea as fuel

0.73), dominant wavelength, lifetime, and color purity are close to values required for displays. Although the quantum yield (0.01) for the prepared samples are lower than standard blue phosphor, factors low persistence and good stability corroborate to phosphor's aplications. Therefore, our results suggest that the combustion method is a promising technique for preparation of blue phosphors to be applied in display technology.

Acknowledgments Authors gratefully thank to Brazilian agencies FAPESP, CNPq and CAPES for financial support.

References

1. Lingdong S, Jiang Y, Changhui L, Chunsheng L, Chunhua Y (2000) Rare earth activated nanosized oxide phosphors: synthesis and optical properties. J Lumin 87–89:447–450
2. Minami T, Utsubo T, Miyata T, Suzuki Y (2003) PL and EL properties of Tm-activated vanadium oxide-based phosphor thin films. Thin Solid Films 445(2):377–381
3. Nakanishi Y, Wada H, Kominami H, Kottaisamy M, Aoki T, Hatanaka Y (1999) Growth and characterization of Y_2O_3:Tm thin-film blue-emitting phosphor. J Eletrochem Soc 146(11):4320–4323
4. Fumo DA, Morelli MR, Segadães AM (1996) Combustion synthesis of calcium aluminates. Mater Res Bull 31(10):1243–1255
5. Gomes J, Pires AM, Serra OA (2002) Blue phosphor prepared by combustion method. Eclética Química 27(n.esp.):187–196
6. Gomes J, Pires AM, Serra OA (2004) Morphological study of Sr_2CeO_4 blue phosphor with fine particles. Quim Nova 27(5):706–708
7. Dasgupta N, Krishnamoorthy R, Jacob KT (2001) Glycol–nitrate combustion synthesis of fine sinter-active yttria. Int J Inorg Mater 3(2):143–149
8. Hao J, Studenikin SA, Cocivera M (2001) Blue, green and red cathodoluminescence of Y_2O_3 phosphor films by spray pyrolysis. J Lumin 93:313–319
9. Dieke GH (1968) Spectra and energy levels of rare earth ions in crystals. Interscience Publishers, New York
10. Rao RP (2005) Tm^{3+} activated lanthanum phosphate: a blue PDP phosphor. J Lumin 113(3/4):271–278
11. Faustino WM, Junior SA, Thompson LC, de Sá GF, Malta OL, Simas AM (2005) Theoretical and experimental luminescence

quantum yields of coordination compounds of trivalent europium. Int J Quantum Chem 103:572–579
12. http://www.colutron.com/products/imaging/pscreen.html
13. International Center for Diffraction Data c. 1998 (CD-ROM) Powder Diffaction File PDF-2 dabase sets 1-44. Pensylvannia Joint Commitee on Powder Diffraction Standards
14. Cullity B (1978) Elements of X-ray diffraction, 2nd edn. Adisson Wesley, Redding
15. Justel T, Nikol H, Ronda C (1998) New developments in the field of luminescent materials for lighting and displays. Angew Chem Int Ed 37(22):3084–3103
16. Santa-Cruz PA, Teles FS (2003) Spectra Lux Software v.2.0 Beta. Ponto Quântico Nanodispositivos, RENAMI
17. Song H, Sun B, Wang T, Lu S, Yang L, Chen B, Wang X, Kong X (2004) Three-photon upconversion luminescence phenomenon for the green levels in Er^{3+}/Yb^{3+} codoped cubic nanocrystalline yttria. Solid State Commun 132(6):409–413